Supplementary Information for

Beautiful Pietàs in South Tyrol (Northern Italy) – local or imported works of art?

Petra Dariz[1], Ulrich Wortmann[2], Jochen Vogl[3], Thomas Schmid[3*]

[1] heritagelab, 39100 Bozen, Italy.
[2] University of Toronto, Department of Earth Sciences, M5S 3B1 Toronto, Canada.
[3] Federal Institute for Materials Research and Testing, Department of Analytical Chemistry; Reference Materials, 12489 Berlin, Germany.

Additional File 2

Results and Discussion

Beautiful Pietàs

Table S1. Mineral phases in the materials composing the Pietàs under study, detected and quantified by powder X-ray diffraction (XRD) analysis performed at the Institute of Geological Sciences of the University of Berne (Switzerland) within the present study (x: <1%; xx: 1% to 10%; xxx: >10%).

Locality	Gypsum	Anhydrite	Calcite	Magnesite	Dolomite	Feldspars	Quartz	Mica/Clay	Celestine	Pyrite
Cathedral Maria Himmelfahrt, Bozen			xxx				x			
Church St. Martin, Göflan	xxx	xxx	xx				x			
Church of Our Lady, Abbey Marienberg	xxx	xx	xx		xx		x		x	
Chapel St. Ann, Mölten	xxx	x	xx		xx	x	x		x	

Beyond the minerals listed in Table S1, hexahydrite $MgSO_4 \cdot 6H_2O$ and high magnesian calcite $(Ca,Mg)CO_3$ were detected in the gypsum mortar samples taken from the Pietà in the Church of Our Lady of the Benedictine Abbey Marienberg and of the Pietà in the Chapel St. Ann in Mölten by Raman microspectroscopy, as described in detail in Ref. [54] and shown in the Figs. 3 and 6 in the main text.

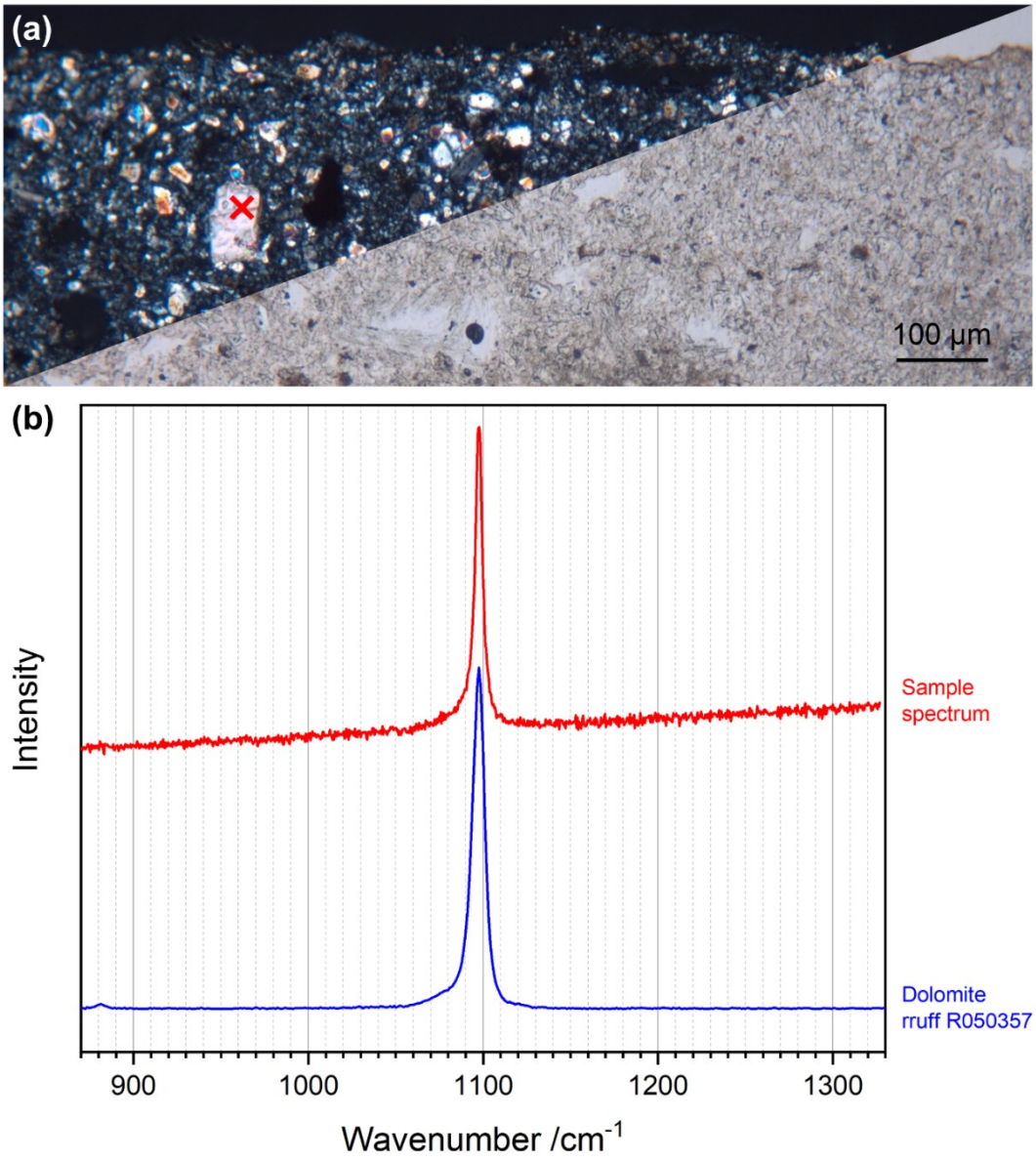

Fig. S1: Sample taken from the Pietà in the Church St. Martin in Göflan: (a) light micrograph (transmitted light, crossed/parallel Nicols), and (b) Raman spectrum acquired at the spot marked with a red cross, enabling the identification of the probed carbonate grain as dolomite $CaMg(CO_3)_2$ (reference spectrum from rruff.info [46]).

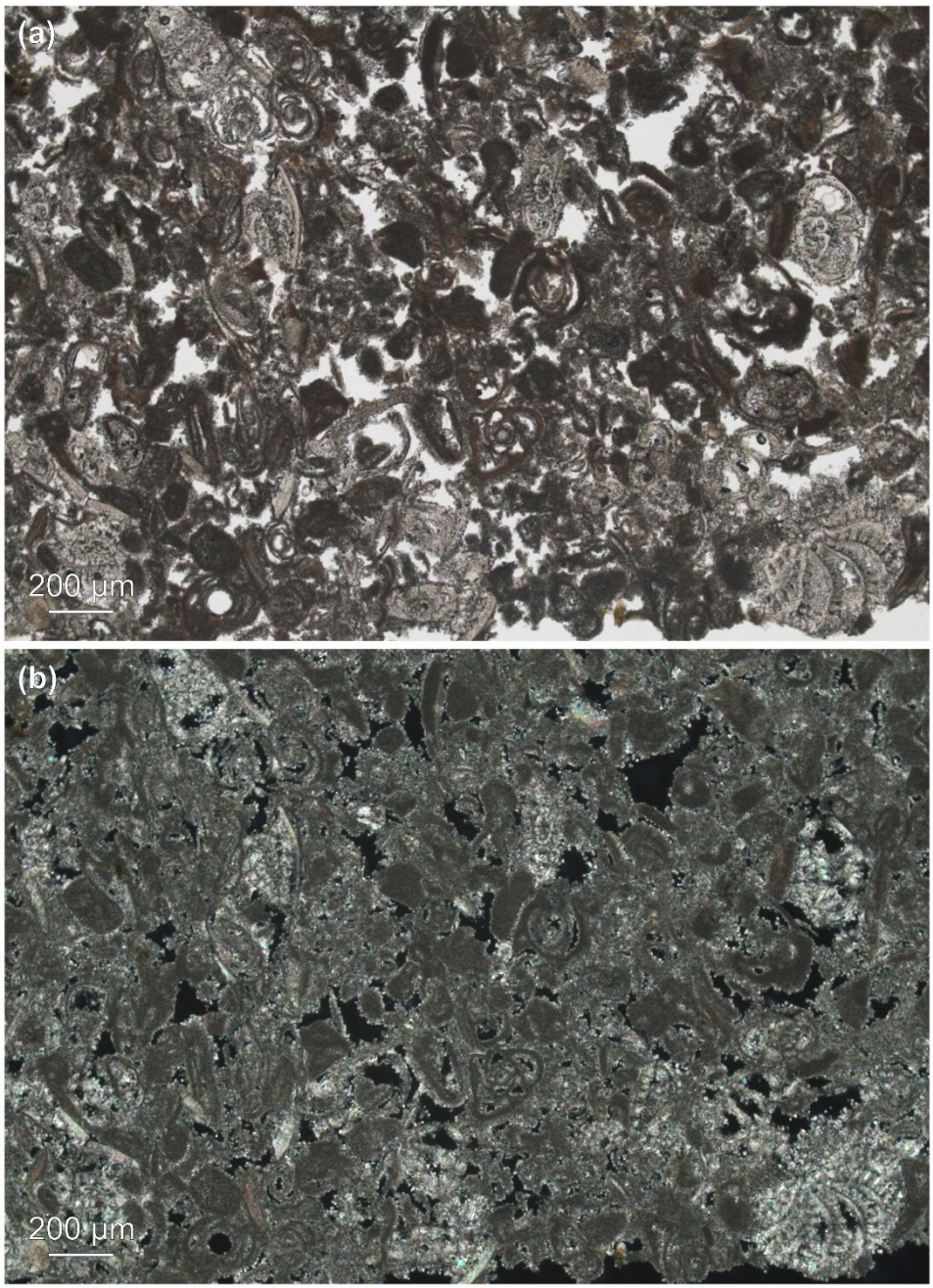

Fig. S2: Light micrographs of the sample taken from the Beautiful Pietà in the Cathedral Maria Himmelfahrt in Bozen made of Breitenbrunn calcareous sandstone (transmitted light, (a) parallel and (b) crossed Nicols).

In view of the distinguishing fine-grained debris of foraminifers, the Beautiful Pietà in the Cathedral Maria Himmelfahrt in Bozen turned out to be made of Breitenbrunn calcareous sandstone (Leitha Mountains, Burgenland, Austria). The designation of Leitha limestones as calcareous sandstones refers to the grain size of the deposited coralline algal debris sand (Rhodophyta, Corallinaceae) or in the case of the abandoned quarry Breitenbrunn of the sedimented foraminiferal sand. Besides the dominating remnants of benthic foraminifera (Orders Miliolida, Textulariida and Rotaliida), fragments of tube worms (Serpulidae), mollusc shells and barnacles (Cirripedia, *Pyrgoma*) can be observed in the thin section of the sample; furthermore, rarely quartz and mica are present. Already macroscopically discernable rust-colored stains are most probably due to the oxidation of glauconite to iron (hydr)oxide [S1–S3].

Gypsum deposits

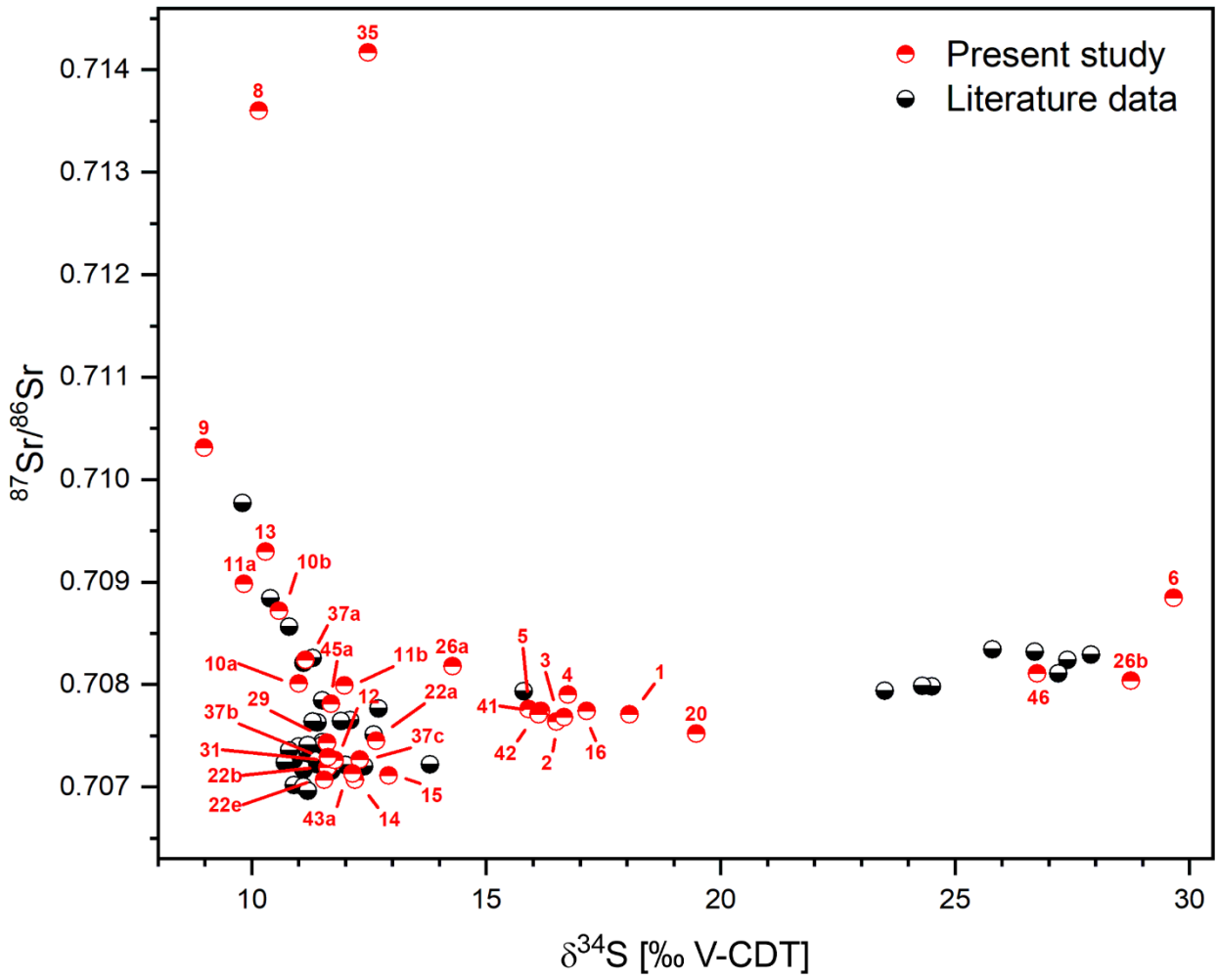

Fig. S3: Graphical representation of all isotopic data evaluated within this study. In contrast to Fig. 9 in the main text, this diagram highlights the isotope values of gypsum deposits in the Eastern Alps, which were measured in the frame of the present study and complement (particularly in the case of strontium isotope values) the currently patchy data situation. The numbers refer to Table 1 and Fig. 9 in the main text as well as Table S2 below, which reveals the mineralogical compositions of the same samples.

Table S2. Mineral phases in gypsum stones from deposits in Switzerland, Italy, and Austria analysed by powder X-ray diffraction (XRD) analysis performed at the Institute of Geological Sciences of the University of Berne (Switzerland) within the present study (x: <1%; xx: 1% to 10%; xxx: >10%).

Locality	No.	Gypsum	Anhydrite	Calcite	Magnesite	Dolomite	Feldspars	Quartz	Mica/Clay	Celestine	Pyrite	Magnetite	Ilmenite	Rutile
Ofenpass (GR, CH)	1	xxx	x	x		xxx	x	x		x				
St. Maria, Val Schais (GR, CH)	2	xxx	x	x		xx		x		x				
Furkelhütte (BZ, IT)	3	xxx	x			xx		x		xx				
Patleigraben (BZ, IT)	4	xxx	x			xx	xx	x	x					
Außertrafoi (BZ, IT)	5	xxx	x			xx				x				
Prissian (BZ, IT)	6	xxx				x		x	xx					
Naifjoch (BZ, IT)	8	xxx	x				x	xxx		x				
Mölten (BZ, IT)	9	xxx					x	x						
San Lugano/Truden (BZ, IT)	10a	xxx		x			x	x		x				
	10b	xxx		x				x		x	x			
Bletterbachschlucht (BZ, IT)	11a	xxx	x				xx	xx						
	11b	xxx		x									x	
Cavalese (TN, IT)	12	xxx		x										
Weißlahn/Aferer Geißler (BZ, IT)	14	xxx	x			xx		x	x					
Tschantschenon (BZ, IT)	15	xxx	x			xx		x						
St. Anton im Montafon (V, AT)	16	xxx	xx					x		x				
Hallein (S, AT)	20	xxx	xxx	x	x		x	x						
Grubach-Moosegg (S, AT)	22a	xxx	x	xx				x						
	22b	xxx	xx	x	xx		x			x				
	22e	xx	xxx	x	xx						x			
Hallstatt (UA, AT)	26a	xxx												
	26b	xxx				xx				x				
Fuchsalm, Spital am Pyhrn (UA, AT)	29	xxx	x		x		xx	x		x				
Weng, Admont (ST, AT)	31	xxx	x	x				x	x	x			x	x
Eisenerz (ST, AT)	35	xxx	x			x	x	xx		x				
Lamingtal, Bruck an der Mur (ST, AT)	37a	xxx	xx	x			x	x	xx					
	37b	xxx	x		xx		xx		x					
	37c	xxx	x		xx		xx	x	x					
Haidbachgraben, Semmering (LA, AT)	41	xxx	x		x		x	x		x		x		
Göstritz (LA, AT)	42	xxx	x							x				
Pfennigbach, Puchberg am Schneeberg (LA, AT)	43a	xxx	x		xx		x			x				
Preinsfeld, Heiligenkreuz (LA, AT)	45a	xxx			xx			x				x		
Mödling (LA, AT)	46	xxx				xxx		x		x		x		

In order to also detect minerals at trace levels, below the detection limit of powder XRD analysis, Raman microspectroscopic mapping experiments of three powdered gypsum stones were performed, which according to their isotope signatures are potential raw materials of the Pietàs in Göflan, and Marienberg/Mölten, respectively. On randomly selected areas, 20 Raman maps of 70 × 70 = 4900 spectra each were acquired, yielding a total number of 98000 spectra for every sample, which were assigned to minerals by comparison with reference spectra from rruff.info [46] or literature data [S4–S6] (Figs. S4–S8).

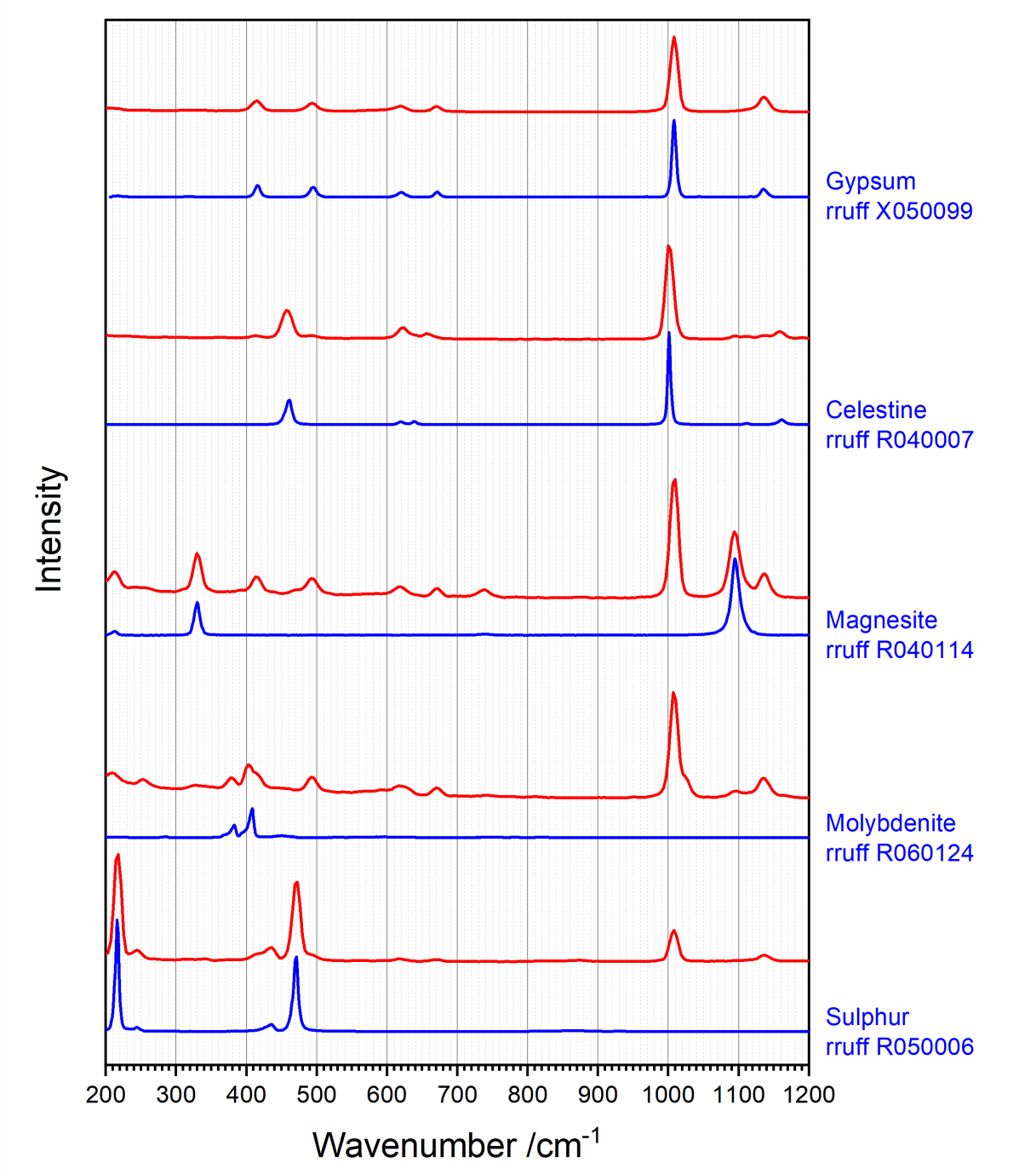

Fig. S4: Minerals detected in a gypsum stone from Grubach-Moosegg (Salzburg, Austria; sample 22b) by Raman microspectroscopy: gypsum $CaSO_4 \cdot 2H_2O$, celestine $SrSO_4$, magnesite $MgCO_3$, molybdenite MoS_2, elemental sulphur S. Note that the spectra of all accessory minerals are superimposed by the spectrum of the major component gypsum.

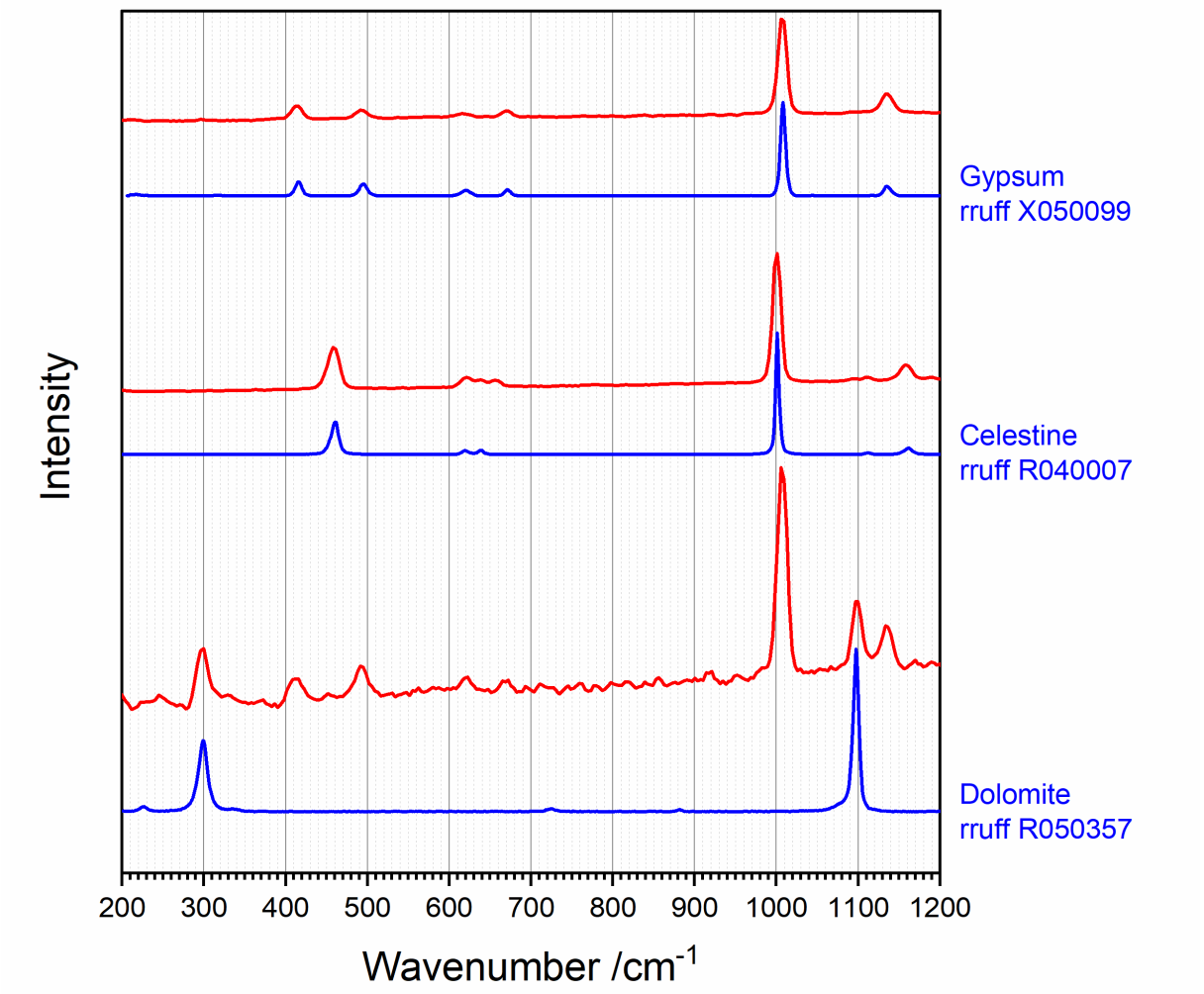

Fig. S5: Minerals detected in a gypsum stone from Hallstatt (Upper Austria, Austria; sample 26b) by Raman microspectroscopy: gypsum, celestine, and dolomite $CaMg(CO_3)_2$. Note that the spectrum of dolomite is superimposed by the spectrum of the major component gypsum.

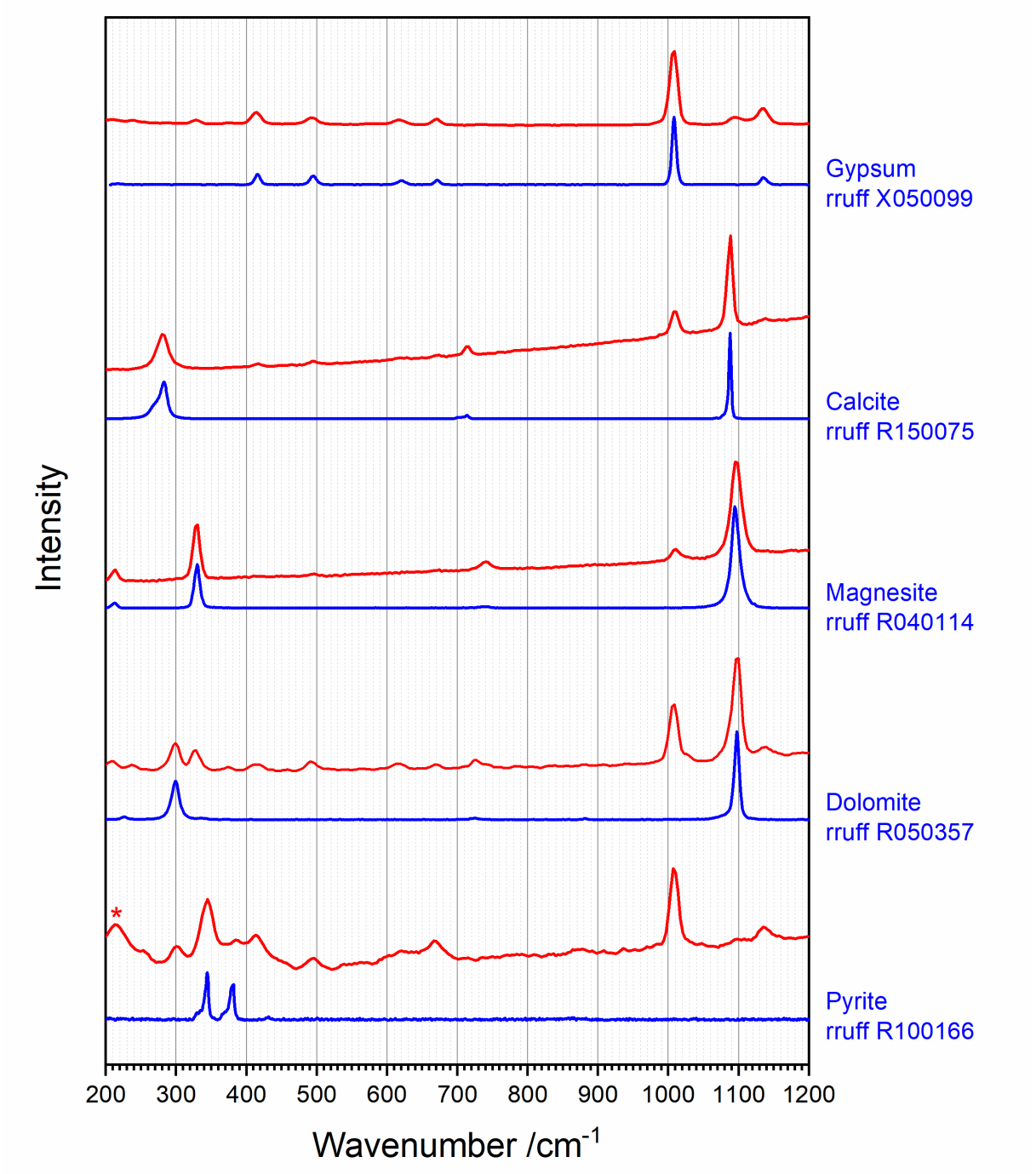

Fig. S6: Minerals detected in a gypsum stone from Pfennigbach (Lower Austria, Austria; sample 43a) by Raman microspectroscopy: gypsum, calcite $CaCO_3$, magnesite, dolomite, and pyrite FeS_2. The band marked with an asterisk (*) additionally confirms the assignment of this spectroscopic signature to pyrite, because indicating partial decomposition of FeS_2 into FeS by the action of the laser beam employed for the Raman measurements [S4]. Note that the spectra of all accessory minerals are superimposed by the spectrum of the major component gypsum.

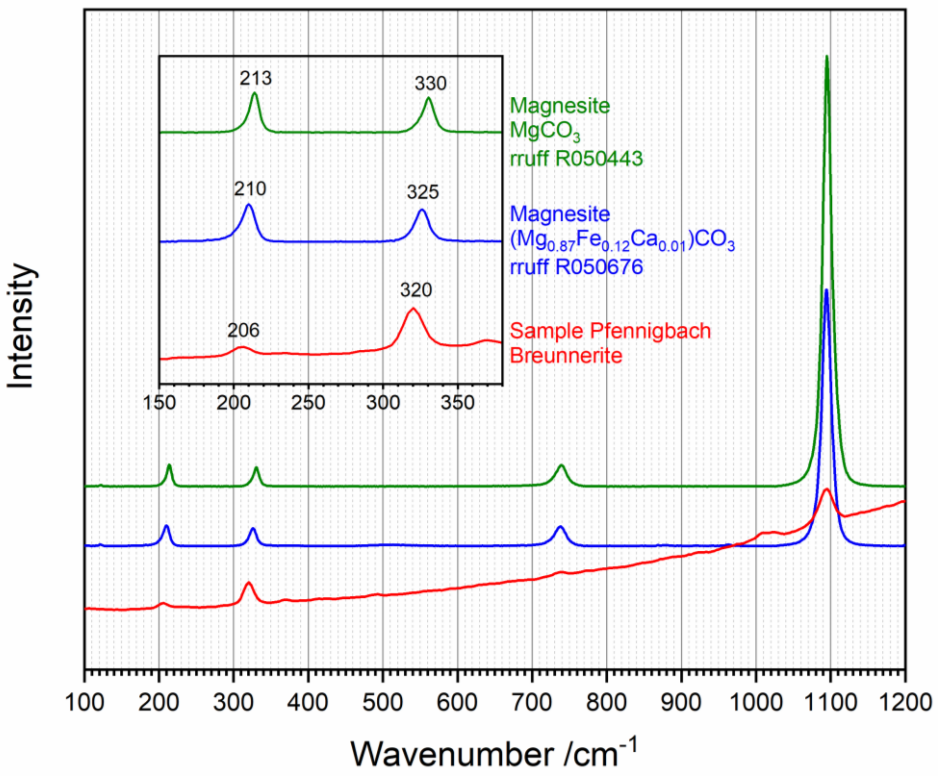

Fig. S7: Raman spectrum acquired in a gypsum stone from Pfennigbach (Lower Austria, Austria; sample 43a) compared to reference spectra of stoichiometric and iron-bearing magnesite. Due to the lack of reference data, the signature is assigned to breunnerite $(Mg,Fe)CO_3$ based on the shown trend of the wavenumbers. Furthermore, a study on Raman band shifts within the solid solution series magnesite–siderite by Nicolas Rividi et al. [S5] points towards a molar Fe:Mg ratio of approx. 30:70, typical for breunnerite. The presence of accompanying breunnerite, mesitine spar or pistomesite (magnesian variety of siderite $FeCO_3$) in Austroalpine gypsum bodies is mentioned by Michael Götzinger/Leopold Weber [58], Christoph Spötl [72, 73], Eberhard Fugger [79] and Elisabeth Kirchner [83].

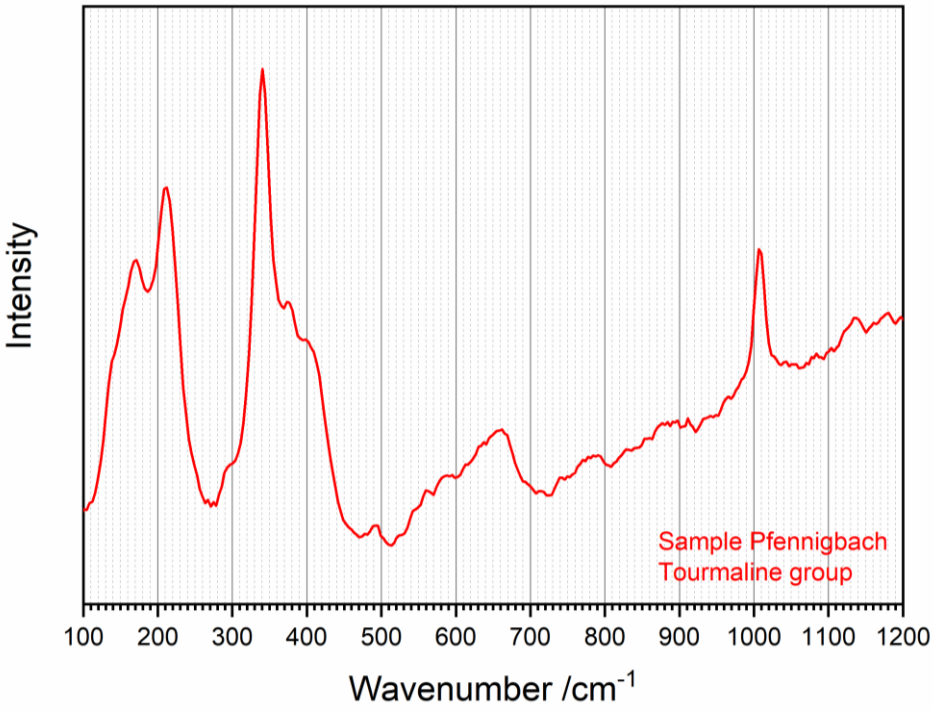

Fig. S8: Raman spectrum acquired in a gypsum stone from Pfennigbach (Lower Austria, Austria; sample 43a) assigned to a tourmaline group member based on reference spectra published by Anke Watenphul et al. [S6].

In addition to the detection of down to trace amounts of accessories in gypsum stones – as shown above for powdered samples –, Raman microspectroscopic imaging of polished thin sections can provide further insight, as for example the visualisation of oxidation rims of haematite around pyrite grains. The phase distribution maps in Figs. S9–S10 elucidate the accompanying minerals of a sample from the local South Tyrolean deposit Furkelhütte, which matches the mineralogical composition of the gypsum mortars of the Pietàs in Marienberg and Mölten, but diverges in terms of its isotope signature (see the wavenumbers of the evaluated marker bands in the Materials and Methods section of the main text).

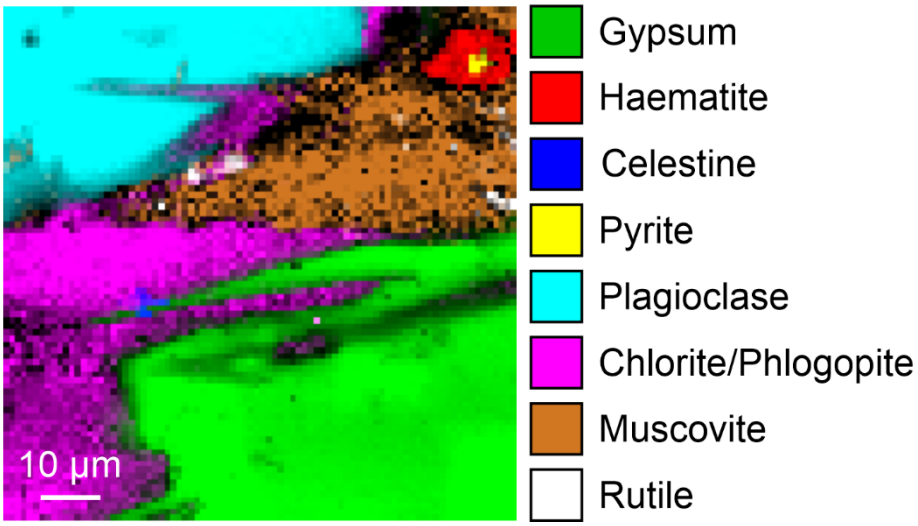

Fig. S9: Raman microspectroscopic intensity map of a gypsum stone from Furkelhütte (South Tyrol, Italy; sample 3) revealing the presence of accompanying feldspar, phyllosilicates (mica- and chlorite-group), pyrite FeS_2 (with oxidation rim of haematite Fe_2O_3), rutile TiO_2, and celestine $SrSO_4$.

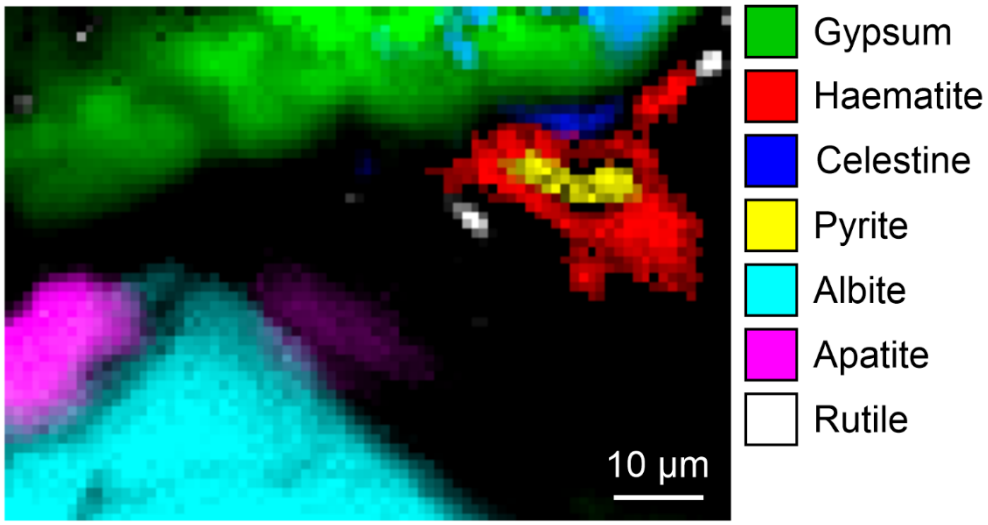

Fig. S10: Raman microspectroscopic intensity map of a gypsum stone from Furkelhütte (South Tyrol, Italy; sample 3) visualising the distribution of the accessories albite $NaAlSi_3O_8$, apatite $Ca_5(PO_4)_3(OH,F)$, pyrite (with oxidation rim of haematite), rutile, and celestine.

References

References in this Supplementary Information labelled [x] (with x denoting a number) refer to the list in the main text, while references of the form [Sx] are used exclusively within the present text and listed below.

[S1] Dullo W-Ch. Fossildiagenese im miozänen Leitha-Kalk der Paratethys von Österreich: Ein Beispiel für Faunenverschiebungen durch Diagneseunterschiede. Facies 1983:8:1–112.

[S2] Flügel E. Mikrofazielle Untersuchungsmethoden von Kalken. Berlin/Heidelberg: Springer-Verlag; 1978.

[S3] Adams A, MacKenzie W. Carbonate sediments and rocks under the microscope. Boca Raton: Taylor & Francis Group; 1998.

[S4] Xi S, Zhang X, Luan Z, Du Z, Li L, Liang Z, Lian C, Yan J. Micro-Raman study of thermal transformations of sulfide and oxysalt minerals based on the heat induced by Laser. Minerals 2019:9:751.

[S5] Rividi N, van Zuilen M, Philippot P, Ménez B, Godard G, Poidatz E. Calibration of Carbonate Composition Using Micro-Raman Analysis: Application to Planetary Surface Exploration. Astrobiology 2010:10:293–309.

[S6] Watenphul A, Schlüter J, Bosi F, Skogby H, Malcherek T, Mihailova B. Influence of the octahedral cationic-site occupancies on the framework vibrations of Li-free tourmalines, with implications for estimating temperature and oxygen fugacity in host rocks. Am. Mineral. 2016:101:2554–2563.